Observations of shock-loaded tin and zirconium surfaces with single-pulse X-ray diffraction

Dane V. Morgan,[a] Mike Grover, Don Macy, Mike Madlener,
Gerald Stevens, and William D. Turley
National Security Technologies, LLC, Los Alamos Operations, 182 East Gate Drive, Los Alamos, New Mexico 87544

(Received 3 March 2010; accepted 9 March 2010)

A single-pulse X-ray diffraction (XRD) diagnostic has been developed for the investigation of shocked material properties on a very short time scale. The diagnostic, which consists of a 37-stage Marx bank high-voltage pulse generator coupled to a needle-and-washer electron beam diode via coaxial cable, produces line-and-bremsstrahlung X-ray emission in a 40 ns pulse. The molybdenum anode produces 0.71 Å characteristic $K\alpha$ lines used for diffraction. The X-ray beam passes through a pinhole collimator and is incident on the sample with an approximately 2 mm × 5 mm spot and 1° full width at half maximum angular divergence. Coherent scattering from the sample produces a Debye-Scherrer diffraction pattern on an image plate located at 75 mm from the polycrystalline sample surface. An experimental study of the polycrystalline structures of zirconium and tin under high-pressure shock loading has been conducted with single-pulse XRD. The experimental targets were 0.1-mm-thick foils of zirconium and tin using 0.4-mm-thick vitreous carbon back windows for shock loading, and the shocks were produced by either Detasheet or PBX-9501 high explosives buffered by 1-mm-thick 6061-T6 aluminum. The diffraction patterns from both shocked zirconium and tin indicated a phase transition into a polymorphic mix of amorphous and new solid phases.
 [DOI: 10.1154/1.3402838]

Key words: X-ray diffraction, shock physics, pulsed X-ray source, zirconium, tin

I. INTRODUCTION

The direct correlation between solid-state structures and their associated X-ray diffraction (XRD) pattern enables single-pulse XRD to provide a unique capability for investigating shocked materials on an atomic scale during the brief time interval that the sample is at high pressure and temperature. Of particular interest are materials such as tin and zirconium, which undergo phase transitions at temperatures and pressures that can be accessed with high-explosive-driven shocks. We have previously studied shock-loaded tin with a small-format image single-pulse XRD system (Morgan *et al.*, 2008) that indicated the existence of a disordered, possibly liquid or amorphous, tin phase at temperatures and pressures where the tin β- and γ-solid-state phases were thought to exist exclusively (Mabire and Héreil, 2000). To substantiate these results, a new series of shock-loaded tin experiments has been performed with an improved large-format imaging single-pulse XRD system. Also, experiments were performed with shock-loaded zirconium to observe the transition from the hexagonal-close-packed (hcp) α phase to the hexagonal ω phase that occurs at pressures around 50 kbar. For pressurized zirconium, the melting point is over 2000 K, a temperature much higher than thought to exist in high-explosive-driven shock experiments, precluding the possibility of melt.

Jamieson (1963) determined a hexagonal structure (ω phase) for pure zirconium at high pressure with XRD, a structure which had previously been reported for zirconium-based alloys by Hatt and Roberts (1960). At pressures above ~350 kbar and at high temperatures, the body-centered-cubic zirconium β phase has been observed by Xia *et al.* (1990, 1991). Zirconium shock experiments have been conducted with a single-pulse XRD diagnostic by Podurets *et al.* (2003) at 0.71 Å using high explosives (HEs). For these experiments, lithium was used as an X-ray window because of its low density and low atomic number. Molybdenum, which was added to the sample to provide a pressure calibration, was observed more strongly in the static diffraction pattern than zirconium. Although observations of a dynamic zirconium phase with 2.11 and 2.27 Å d spacings were reported, the poor signal-to-noise ratio and 1° to 2° angular scattering resolution adversely affected the measurement. Also, the molybdenum (110) line at room temperature and pressure has a planar spacing of 2.23 Å, which compresses to about 2.19 Å at 150 kbar, making resolution of these zirconium lines extremely difficult. The pulse width of the source used by these authors was approximately 200 to 300 ns, which likely caused motion blur in the dynamic image. Furthermore, significant structural transformations may have occurred during the extended X-ray pulse time.

At room temperature and pressure, tin exists in a "diamondlike" tetragonal β phase, which undergoes a high-pressure solid-solid phase transition to the simple body-centered-tetragonal (bct) γ phase first identified by Barnett *et al.* (1963). Later, the $\beta \rightarrow \gamma$-phase change boundary was carefully measured with XRD in temperature-pressure space and the γ-phase bct c/a ratio was found to be 0.912 ± 0.002, varying only slightly along the phase transition boundary (Barnett *et al.*, 1966). Mabire and Héreil (2000) reported dynamic solid-state $\beta \rightarrow \gamma$ and $\gamma \rightarrow \beta$ shock-induced phase transformations in tin using a velocity interferometry system for any reflector (VISAR); Buy *et al.* (2006) achieved the same results using a plate impactor, and Davis and Hayes

[a]Author to whom correspondence should be addressed. Electronic mail: morgandv@nv.doe.gov

(2007) detected the transformations under magnetic pressure loading. The transformations were identified by discontinuity of the interface velocity and by acceleration in the velocity profile, events that occurred in time intervals of a few nanoseconds. However, because VISAR measurements alone cannot uniquely identify solid-state phases, a superset of static high-pressure, high-temperature XRD data was used to form hypotheses for the new structures that were indicated by VISAR. The tin $\beta \rightarrow \gamma$ structural and volumetric transformations of the individual tin grains may only be inferred from VISAR data, and dynamic single-pulse XRD data should provide insight to the dynamic tin behavior during the phase transition at the atomic level.

The results of a series of high-explosive-driven shock-loaded polycrystalline experiments performed on tin and zirconium samples in a high-pressure, high-temperature dynamic state using a single-pulse XRD diagnostic are reported here. The purpose of these experiments was to observe the structures of tin and zirconium during shock loading to determine the structures that exist while increased pressures and temperatures were slowly varying with time. Material properties, including texture and grain size distribution, were also investigated.

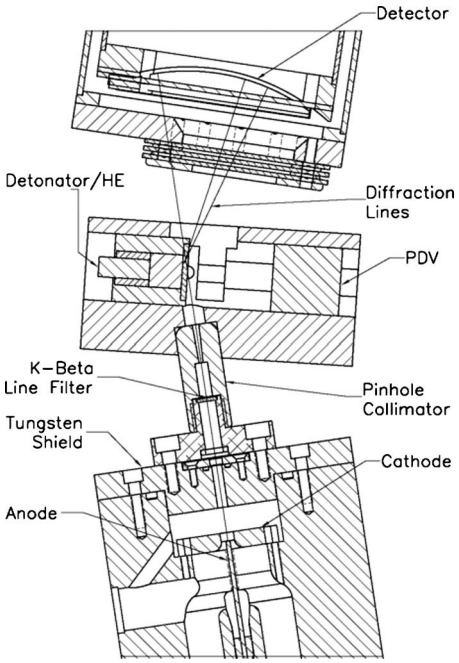

Figure 1. Single-pulse XRD experimental configuration. The collimated line-and-bremsstrahlung source is incident on the target sample. The line emission diffracted from the sample surface and the hard bremsstrahlung direct beam were recorded on the image plate detector.

II. EXPERIMENTAL

Characteristic $K\alpha$ X-rays used for single-pulse XRD in these experiments were conventionally produced by a 37-stage high-voltage Marx pulse generator coupled to a vacuum needle-and-washer X-ray diode via coaxial transmission line. The Marx pulse generator, described previously (Morgan *et al.*, 2008), delivered a 40 ns pulse to the X-ray diode with a timing uncertainty of less than 10 ns. The estimated peak voltage across the anode-cathode gap in the X-ray diode was approximately 400 kV. Electron impact on a 1.5-mm-diameter needle-shaped anode of molybdenum produced a large amount of continuum bremsstrahlung X-rays, as well as the 0.71 Å molybdenum characteristic fluorescent line that is utilized for XRD. A 1.5-mm-diameter tungsten pinhole collimator with a 4° full-angle conical taper produced a narrow beam of X-rays incident on the sample axis with about 1° divergence. An electromagnetic pickup near the diode measured the X-ray pulse timing.

A large field-of-view X-ray detection system utilizing a Fuji BAS-MS image plate was developed for these experiments to enable observation of the entire diffraction pattern. A film holder, placed inside a blast protection system, could be inserted and removed to the same position for static and dynamic XRD images. The film holder fixture held the cylindrically bent image plate at a radius of 75 mm. The geometric axis of the image plate cylinder bisected the axis of the target package at the surface of the sample under study as shown in Figure 1. To obtain a large field of view, a blast protection system was developed to mitigate the possibility that debris from the high-explosive-driven experiments would damage the image plate. A steel-tube reentrant inside the experimental chamber supported a tungsten plate that served as both a blast protection shield and beam attenuator. At the location where the direct beam was incident on the tungsten blast shield, the tungsten thickness was reduced to 3.8 mm to allow a small portion of the hard bremsstrahlung within the beam to expose the image plate, providing a method for precise determination of the scattering angles. A 40-mm-diameter window in the tungsten plate allowed scattered X-rays from the sample to reach the image plate. This window was protected by multiple layers of rigidly mounted high-density polyethylene separated by small air gaps.

The experiments were conducted at the High Explosives Facility at NSTec's Special Technologies Laboratory. The entire single-pulse XRD diagnostic was installed on the high-explosive chamber's two large opposing ports inside high-explosive containment hardware. The vacuum X-ray diode was located inside a blast containment tube, with specially designed high-voltage coaxial and vacuum feed-throughs that allowed placement of the X-ray source very close to the sample. Both Detasheet and PBX-9501 HEs were used in the experiments. Data from a photonic Doppler velocimeter diagnostic were used to determine the timing of the shock breakout with respect to the X-ray pulse, and the free surface velocity data were used to infer the location and pressure of the shock-loaded interface at the X-ray pulse time.

III. RESULTS AND DISCUSSION

A. Tin

Experiment 080616-1 was performed to study the dynamic properties of shocked tin and in particular to verify previous observations of a broad interference peak associated with a lack of repeating structure (Morgan *et al.*, 2008). This experiment was conducted with a thin 0.1 mm sheet of tin sandwiched between the 1 mm 6061-T6 aluminum buffer and a 0.4 mm vitreous carbon back window driven by Detasheet HE. Diffraction X-rays were generated with a fil-

https://doi.org/10.1154/1.3402838 Published online by Cambridge University Press

TABLE I. Summary of dynamic experiments.

Experiment No.	Configuration	X-ray delay from interface shock arrival (ns)	λ (Å)	Peak interface pressure (kbar)	Release pressure (kbar)
080616-1	Al:Sn:C	115	0.71	194	64
080707-2	Al:Zr:C	80	0.71	329	108
080708-1	Al:Zr:C	96	0.71	335	110

tered molybdenum anode at a wavelength of 0.71 Å. The experimental timing, peak pressure, and reduced pressure as calculated by the WONDY code for experiment 080616-1 are shown in Table I. The X-ray pulse was incident on the sample interface approximately 115 ns after the initial shock arrival.

The room-temperature β-phase tin structure is a face-centered-tetragonal structure with a lattice constant of 3.21 Å and c/a ratio of 0.546. A second identical lattice is offset at coordinates $(a,a,c)/4$, resulting in a diamondlike tetragonal structure. The static image of the β-phase tin structure in Figure 2(a) shows the resolved reflections of the sample's individual tin grains. The dynamic image shown in Figure 2(b) reveals the broad interference peak reported previously (Morgan *et al.*, 2008) with a linewidth and scattering angle consistent with the tin first interference peak reported by Vahvaselkä (1978). Also observed in this image are weak Debye-Scherrer rings composed of granular reflections that indicate the presence of solid material with a reduced grain size. A comparison of the experiment 080616-1 static and dynamic XRD patterns corrected for interface motion is shown in Figure 3. The strong unresolved (311) and (400) diffraction lines in the static diffraction pattern virtually disappear in the dynamic image. Although the dynamic scattering from tin is dominated by the broad interference peak associated with a disordered state, the dynamic image gives trace evidence for a new solid phase. Two weak diffraction lines, clearly distinguishable from any possible residual β-phase material, appear in the dynamic diffraction pattern in Figure 3. The γ-phase tin (101) and (110) cannot be resolved by our single-pulse XRD system, and Barnett *et al.* (1966) showed that the (101) line is considerably more intense. The observed dynamic diffraction lines in Figure 3 are consistent with the (101) and with the (200) γ-phase tin reflections. WONDY calculations indicate that the tin is held at an elevated temperature of about 480 K at the time of the X-ray measurement.

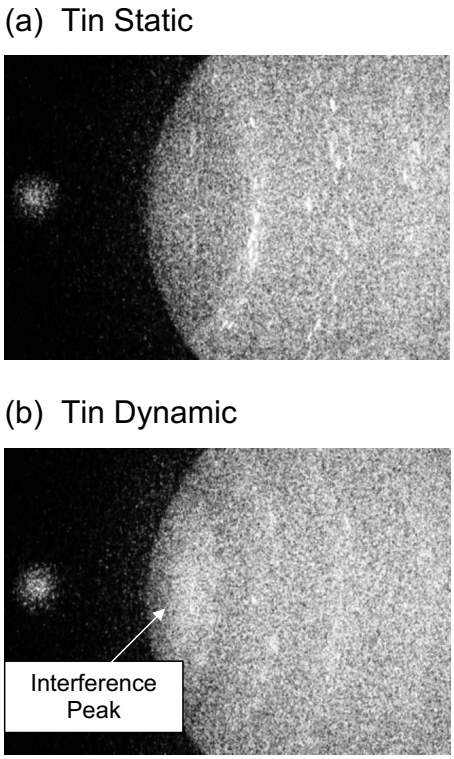

Figure 2. (a) Static and (b) dynamic single-pulse XRD images observed for shock-loaded tin from experiment 080616-1.

B. Zirconium

The experimental configuration for zirconium experiment 080707-2 described in this article was the same as the configuration for tin, with the exception that PBX-9501 HE was used instead of Detasheet, generating a considerably higher shock pressure. Diffraction X-rays for the zirconium experiments were 0.71 Å. Figure 4(a) shows an hcp-structured zirconium single-pulse XRD image at room temperature and pressure. For experiment 080707-2, the zirconium sample was shocked to a peak pressure of 329 kbar; the observed dynamic image is shown in Figure 4(b). The dynamic zirconium image, as had tin, shows a broad interference peak at low scattering angles, which is indicative of scattering from a phase with no repeating structure. Three

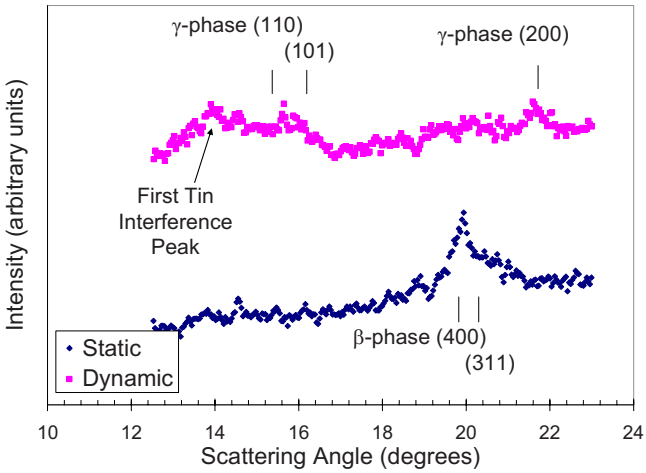

Figure 3. (Color online) Comparison of static and dynamic integrated intensities for shock-loaded tin from experiment 080616-1, showing the transition to a solid and amorphous mixed phase. The γ-phase scattering angles are inferred from Barnett *et al.* (1966).

https://doi.org/10.1154/1.3402838 Published online by Cambridge University Press

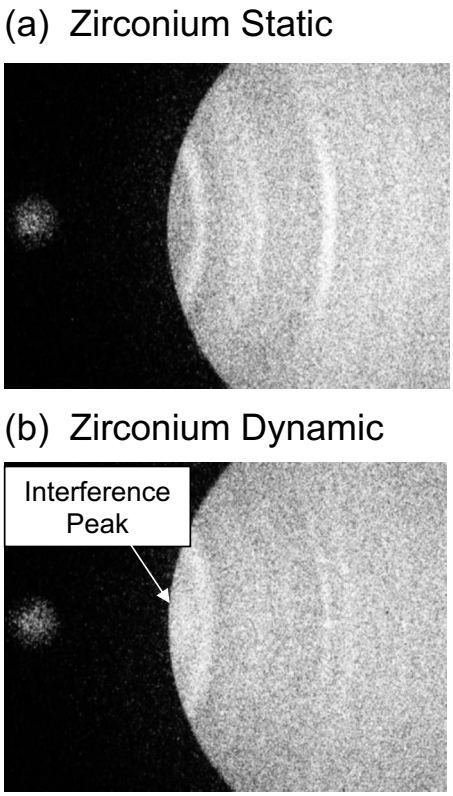

Figure 4. (a) Static and (b) dynamic single-pulse XRD images observed for shock-loaded zirconium from experiment 080707-2.

solid-state diffraction lines are also clearly present, and weaker lines are discernable just above the background.

Integrations of the zirconium static and dynamic diffraction images in Figure 4 with correction for interface motion are shown in Figure 5. The static diffraction lines are compared with the established diffraction scattering angles for the hcp structure with values of 5.146 and 3.233 Å for c and a, respectively. Figure 5 also shows a comparison of the observed dynamic lines with the hexagonal ω-phase high-pressure cell measurements at 109.7 kbar. At this high pressure the lattice parameters reported by Zhao *et al.* (2005) are

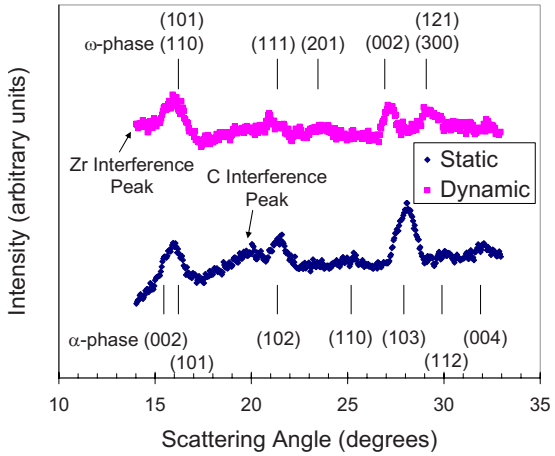

Figure 5. (Color online) Comparison of static and dynamic integrated intensities for shock-loaded zirconium from experiment 080707-2 showing the transition to a solid and amorphous mixed phase. The ω-phase scattering angles are from Zhao *et al.* (2005).

3.031 and 4.872 Å for c and a, respectively. Discrepancies may exist because of the elevated temperature of the shocked zirconium sample and the uncertainty of the inferred experimental pressure; however the predicted location of the hexagonal ω-phase peaks agrees quite well for the strongest peaks observed in the dynamic single-pulse XRD pattern. A second zirconium experiment, designated experiment 080708-1, performed with identical initial parameters with slightly increased delay time (96 ns), gave essentially the same dynamic XRD pattern, thereby confirming the results of experiment 080707-2. The dynamic shock-loaded zirconium lines reported by Podurets *et al.* (2003) were not observed.

IV. CONCLUSION

Shock-loaded tin driven to peak pressures above 194 kbar transforms to a liquid-solid mixed phase upon release to a reduced pressure around 64 kbar, 115 ns after the initial shock reaches the interface. The weak reflections from the new solid γ-phase tin indicate a grain size smaller than the static β-phase tin.

For the zirconium $\alpha \rightarrow \omega$ transition, the ω-phase solid-state diffraction lines are clearly identified. Furthermore, a zirconium liquid diffraction peak is evident, while the experimental temperature is much lower than the melt temperature. These results describe a dynamic model for solid-solid phase transitions for which a large fraction of the atoms are observed to be in the process of diffusing to new lattice sites in the sample shortly ($\sim$100 ns) after the material is shocked and held under stress.

ACKNOWLEDGMENTS

This article has been authored by National Security Technologies, LLC, under Contract No. DE-AC52-06NA25946 with the U.S. Department of Energy. The United States Government retains and the publisher, by accepting the article for publication, acknowledges that the United States Government retains a nonexclusive, paid-up, irrevocable, worldwide license to publish or reproduce the published form of this article or allow others to do so for United States Government purposes.

Barnett, J. D., Bean, V. E., and Hall, H. T. (**1966**). "X-ray diffraction studies on tin to 100 kbar," J. Appl. Phys. **37**, 875–877.

Barnett, J. D., Bennion, R. B., and Hall, H. T. (**1963**). "X-ray diffraction studies on tin at high pressure and high temperature," Science **141**, 1041–1042.

Buy, F., Voltz, C., and Llorca, F. (**2006**). "Thermodynamically based equation of state for shock wave studies: Applications to the design of experiments on tin," in *Shock Compression of Matter–2005*, edited by M. D. Furnish, M. Elert, T. P. Russell, and C. T. White (American Institute of Physics, Melville), pp. 41–44.

Davis, J. and Hayes, D. B. (**2007**). "Measurement of the dynamic β-γ phase boundary in tin," in *Shock Compression of Condensed Matter–2007*, edited by M. Elert, M. D. Furnish, R. Chau, N. Holmes, and J. Nguyen (American Institute of Physics, Melville), pp. 159–162.

Hatt, B. A. and Roberts, J. A. (**1960**). "The ω-phase in zirconium base alloys," Acta Metall. **8**, 575–584.

Jamieson, J. C. (**1963**). "Crystal structures of titanium, zirconium, and hafnium at high pressure," Science **140**, 72–73.

Mabire, C. and Héreil, P. L. (**2000**). "Shock induced polymorphic transition and melting of tin up to 53 GPa (experimental study and modeling)," J.

Phys. IV **10**, 749–753.
Morgan, D. V., Macy, D., and Stevens, G. (**2008**). "Real time X-ray diffraction measurements of shocked polycrystalline tin and aluminum," Rev. Sci. Instrum. **79**, 1–6.
Podurets, A. M., Dorokhin, V. V., and Trunin, R. F. (**2003**). "X-ray diffraction study of shock-induced phase transformations in zirconium and bismuth," High Temp. **41**, 216–220.
Vahvaselkä, K. S. (**1978**). "X-ray diffraction analysis of liquid Hg, Sn, Zr, Al and Cu," Phys. Scr. **18**, 266–274.
Xia, H., Duclos, S. J., Ruoff, A. L., and Vohra, Y. K. (**1990**). "New high-pressure phase transition in zirconium metal," Phys. Rev. Lett. **64**, 204–207.
Xia, H., Ruoff, A. L., and Vohra, Y. K. (**1991**). "Temperature dependence of the ω-bcc phase transition in zirconium metal," Phys. Rev. B **44**, 10374–10376.
Zhao, Y., Zhang, J., Pantea, C., Qian, J., and Daemen, L. L., (**2005**). "Thermal equations of state of the α, β, and ω phases of zirconium," Phys. Rev. B **71**, 184119.

https://doi.org/10.1154/1.3402838 Published online by Cambridge University Press